Simulation of the flow around a Vertical Axis Wind Turbine :

LS-DYNA® v980

Iñaki CALDICHOURY[(1)], Vincent LAPOUJADE[(1)], Hervé LE SOURNE[(2)], Abdelhaq ABDELQARI[(2)], Facundo DEL PIN[(3)]

(1) Alliance Services Plus (AS+), Toulouse, France

(2) Institut Catholique d'Arts et Métiers (ICAM), Nantes, France

(3) Livermore Software Technology Corporation (LSTC),Livermore, U.S.A

Abstract:

The future 980 version of LS-DYNA® will include Computational Fluid Dynamics (CFD) solvers. The main objective of these new solvers will be to perform fluid structure interactions by directly solving the Navier-Stokes equations and by using any LS-DYNA® Lagrangian model for the solid part. In the process of evaluating the new possibilities offered by these new solvers, in particular concerning fluid structure interaction, AS+ has worked in partnership with both industrial and academic clients on the case of a vertical axe wind turbine which was used in the French around the world boat race "Vendée Globe".

The final objective of these simulations is to test various turbine shapes and airfoils in order to determine which one would offer the best aerodynamic behavior without any compromise to its structural behavior. Tests were therefore first conducted on static or oscillating airfoils. Then, 2D simulations of various turbine shapes were performed before aiming for the complete 3D simulation of the problem.

This paper aims to highlight the main features of the new incompressible solver by presenting the results obtained on one of the first industrial cases that use the new v980 version.

Figure 1 Darrieus Wind Turbine Embarked on R. Dinelli's Sailing Boat During the "Vendée Globe" World Boat Race

Introduction:

When Raphaël Dinelli, a notorious French skipper, decided to participate in the 2009th edition of the French *Vendée Globe* sailing race, he didn't think of reaching first place, but had rather decided to pursue a different objective: proving that it could be possible to complete a world tour by boat, and by being totally independent regarding electricity uses on board. In order to reach this goal, he used solar panels and a Vertical Axe Wind Turbine (VAWT) (see figure 1).

A helicoidally Darrieus wind turbine was customized and reinforced with the objective to sustain the difficult conditions encountered during such a race. Now, the next step was to increase its electrical yield by improving the devices (generator, regulator etc…) and carefully choosing the airfoil shapes of the blades.

Through the organization he founded in 2007, Ocean Vital Foundation, he contacted ICAM Nantes, a French engineering school, in order to see what results could be achieved through numerical simulation. ICAM Nantes has in turn, contacted AS+ in order to establish a partnership and to work on the beta version of the future 980 version of LS-DYNA.

Indeed, the future CFD solvers that will be included in LS-DYNA aim to solve complete fluid-structure interaction problems that would then be perfectly suited in order to simulate the complex interactions between the wind flow and the turbine's structure.

This paper will therefore present the different steps that will be completed during the study as well as presenting the first results obtained during the validation process of these new solvers.

Choice of the Turbulence Model:

The main objective of the new CFD solvers, that will be implemented in the future 980 version of LS-DYNA, is to handle fluid structure interactions by correctly and precisely solving the Navier-Stokes equations.

The choice of the turbulence model is therefore essential in order to correctly simulate the behavior of the boundary layer and predict such complex phenomena as laminar-turbulent transition or boundary layer separation point.

The incompressible solver offers three turbulence models:

- A RANS model, the k-ε model which is one the most widely used turbulence model. It is a two equations model meaning that it includes two extra transport equations; one for the turbulent kinetic energy '**k**' and one for the dissipation '**ε**'**,** to represent the turbulent properties of the flow [1]. The different constants associated with the model will be left by default for our tests.

- A LES model, the Smagorinsky model. As the power of computers increases, LES models have become a popular technique in order to simulate turbulence. It is based on Kolmogorov's assumption that large eddies depend on the geometry while smaller eddies are more universal. Therefore LES models will apply a filter on the flow explicitly solving large eddies while simulating smaller ones. The Smagorinsky model used here is one of the most common LES models.

- A VMS model for Variational Multiscale. This model is based on some recent research stating that the rate of transfer of subgrid kinetic energy provided by the stabilization terms of the Orthogonal Subgrid Scale (OSS) finite element method is already proportional to the molecular physical dissipation rate (for an appropriate choice of the stabilization parameter) and that no additional turbulence model should be used. This argument will only be valid for a particularly fine mesh [2].

In order to test the various turbulence models, we have reproduced some experimental recordings of the flow over a NACA 0012 airfoil [3]. These experimental results have been obtained though Particle Image Velocimetry which is known to produce accurate measurements and will therefore be considered as being the reference for our tests.

The first series of tests consisted in reproducing the flow over a NACA 0012 airfoil with a 4.9 angle of attack, a 10 m/s incoming velocity and a 5.4e4 chord length based on Reynolds Number. We decided to test the various turbulence models with the finest meshing that would provide an acceptable calculation time on our machines i.e. 1200 elements for the airfoil and an element size of 0.012 m for the computation domain boundaries. Based on the chord length, we also chose our computational domain large enough in order to consider the different boundary conditions valid (Velocity inlet, Pressure Outlet) (Figure 2):

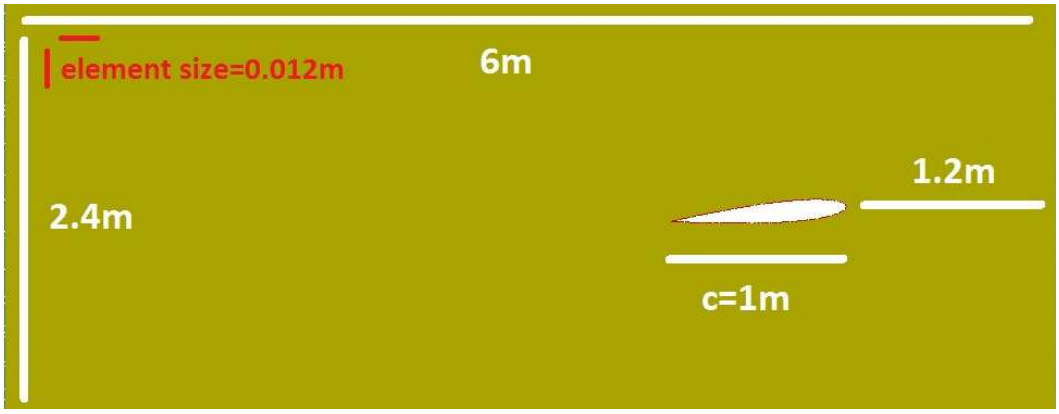

Figure 2 Computational Domain

The incompressible solver also allows adding some elements to the boundary layer before automatically meshing the fluid volume (Figure 3).

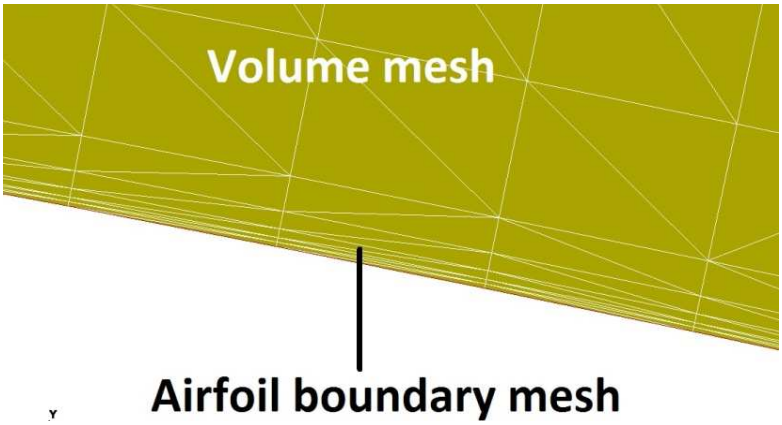

Figure 3 Boundary Layer Meshing

The pressure coefficients obtained by using three turbulence models are then compared to experimental ones and shown in the figure below:

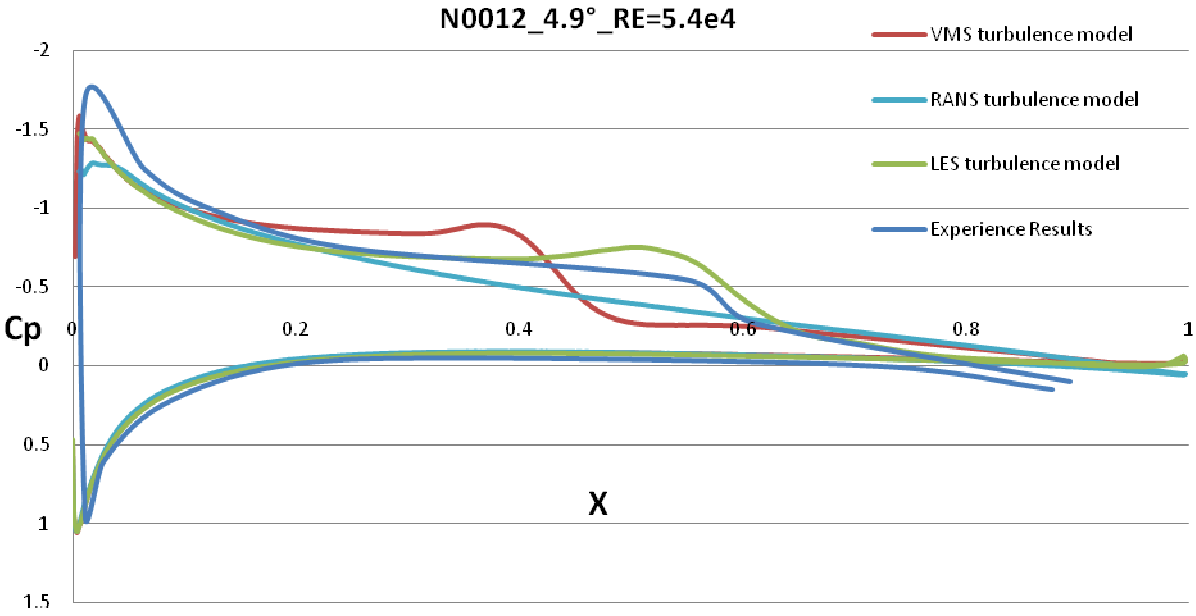

Figure 4 Results on the Cp for Different Turbulence Models

Comments:

- The results on the last ten percents of the chord length have not been measured during the experience. That is why that part of the curve will not be studied here.

- The behavior of the flow around the lower camber is correctly reproduced for the three turbulence models; we will therefore focus on the results of the upper camber.

- The maximum depression zone occurring at the beginning of the upper camber is captured for all three turbulence models but systematically underestimated (by ≈5% for the VMS model, 10% for the LES model, 25% for the RANS model). Consequently the Cl/Cd ratio values are underestimated by about 15% to 20% for all turbulence models and won't be considered as criteria for the comparison of the turbulence models.

- The phenomenon that interests us the most here is the capturing of the sudden raise in pressure that occurs at X = 0.5425 and which correspond to the laminar-turbulent transition of the boundary layer [3]. As we are studying the various turbulence models, this transition point will be considered as our reference point. The VMS and LES models both seem to be able to capture this transition occurring, but the RANS model does not. We will therefore from now on focus on the VMS and LES models.

- Before reaching the transition point and the significant rise in pressure, for both the LES and VMS models, one can spot a little drop in pressure. After visualization of the flow's pressure, we noticed that this was due to the fact that the turbulent transition caused the formation of depression bubbles that, at the point where they are created, influence the pressure values on the airfoil therefore causing this little drop (Figure 4).

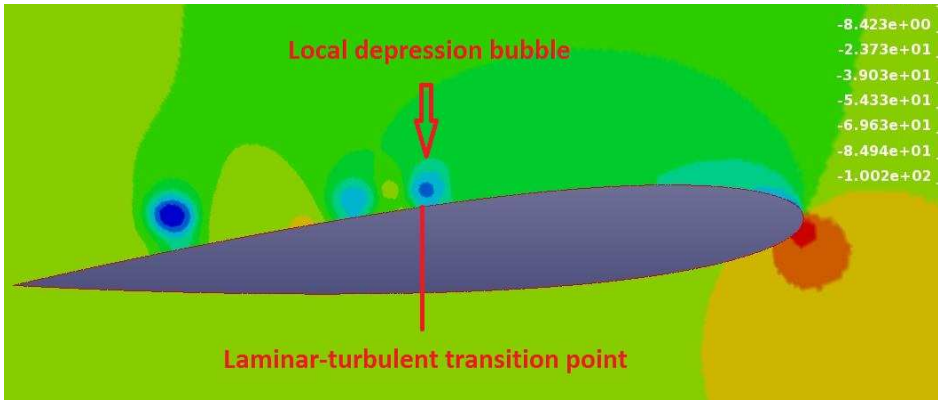

Figure 5 Pressure Visualization of the Flow

If one chooses to ignore this drop and to filter the curve, the results obtained for the Cp curves are shown below:

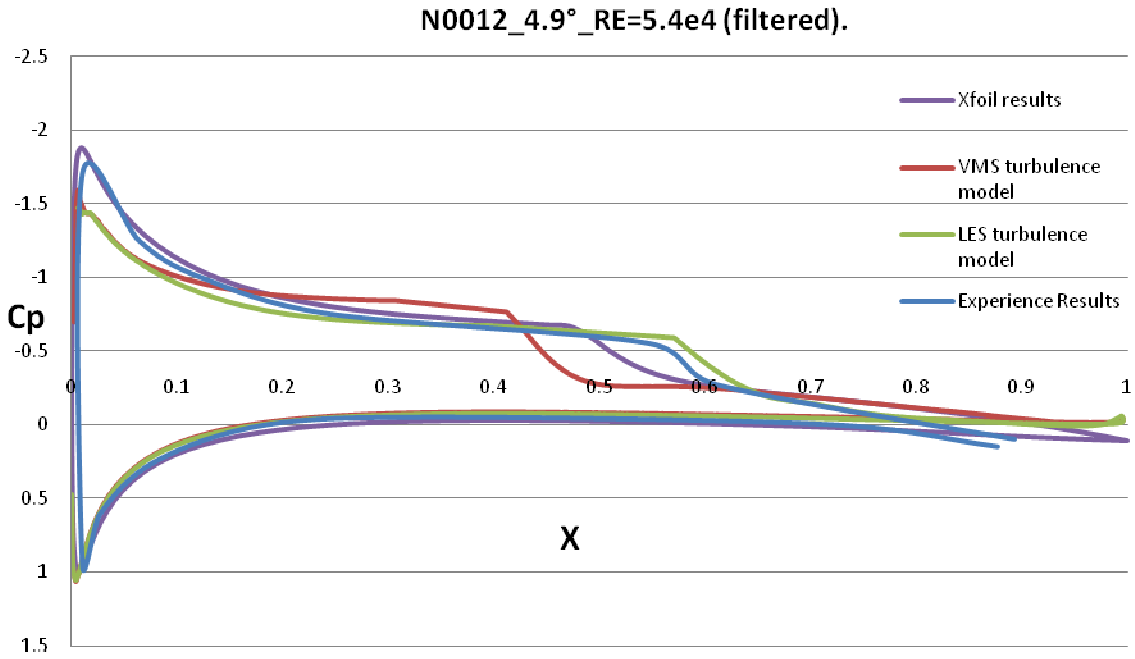

Figure 6 Comparison of the Cp Behavior once Filtered for Different Turbulence Models

We also chose to add the results given by X-foil, software that calculates the pressure coefficients of airfoils based on paneling methods for inviscid flows and by adding extra analytical corrections to simulate the behavior of boundary layers. The result given here by X-foil uses the default value of Ncr=9. As we can see, the LES model offers more accurate results.

	RANS	LES	VMS	X-foil
Laminar-turbulent transition captured	**NO**	**YES**	**YES**	**YES**
Laminar-turbulent transition point position	**-**	**0.574**	**0.417**	**0.47**
Error (%) when comparing to experiment	**-**	**5.8%**	**37%**	**13%**

Table 1 Comparison of the Results for Different Turbulence Models

From this NACA airfoil analysis, , we chose to use the LES turbulence model for the wind turbine study because it gives the most accurate results in the prediction of subtle phenomena such as laminar-turbulent transition.

Mesh Size Convergence Analysis

Once the turbulence model that gave the best results has been identified, we analyzed the influence of the mesh size on the previously obtained results.

We chose to run several calculations based on the number of nodes that discretize the airfoil. In order to always keep a grid refinement factor close to 1.3, we chose to run the test cases for different number of nodes: 350, 550, 720, 820, 920, and 1200. We got the following error percentage evolution based on the experimental result:

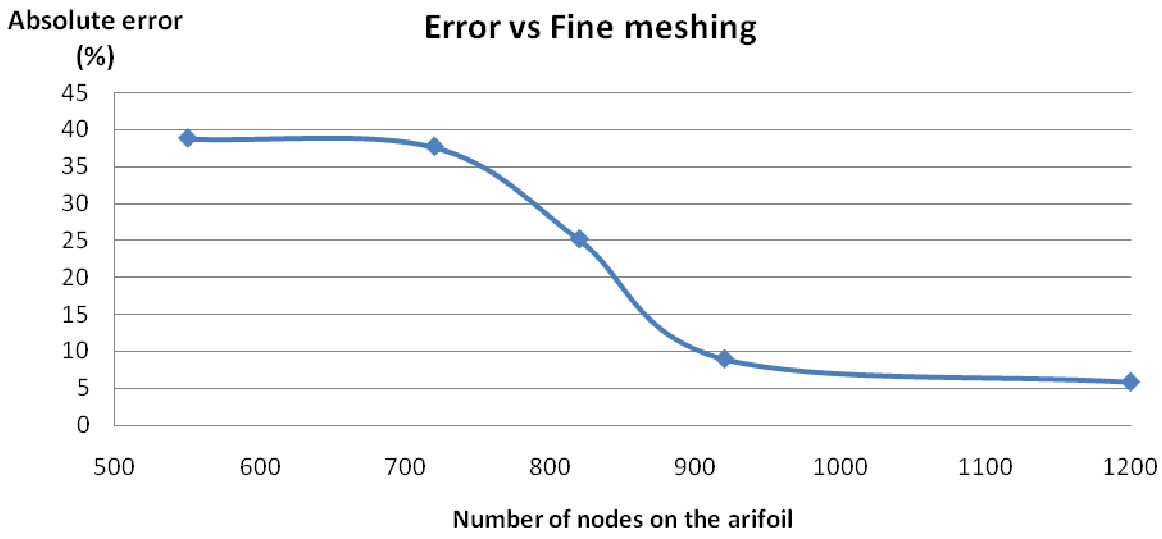

Figure 7 Approximate Absolute Errors as a Function of Mesh Refinement

Figure 7 shows that between 550 nodes and 1200 nodes, the error has been divided by 6 for a grid refinement factor of 2.2. Furthermore, the drop in the error value is sudden with a huge error diminution between 720 and 920 nodes (error divided by 4 with a grid refinement factor of around 1.3). It is therefore crucial for our future studies to be very careful about the mesh size of the chosen

airfoils in order to correctly capture and simulate the laminar turbulent transitions. It seems prudent to use a number of nodes of around one thousand in order to get an acceptable error value.

Using the 350 nodes airfoil model, the laminar turbulent transition was no longer captured, which further emphasizes the need for a fine mesh.

The following figure shows the behavior of the Cp curves obtained for three different numbers of nodes: 550, 820 and 1200.

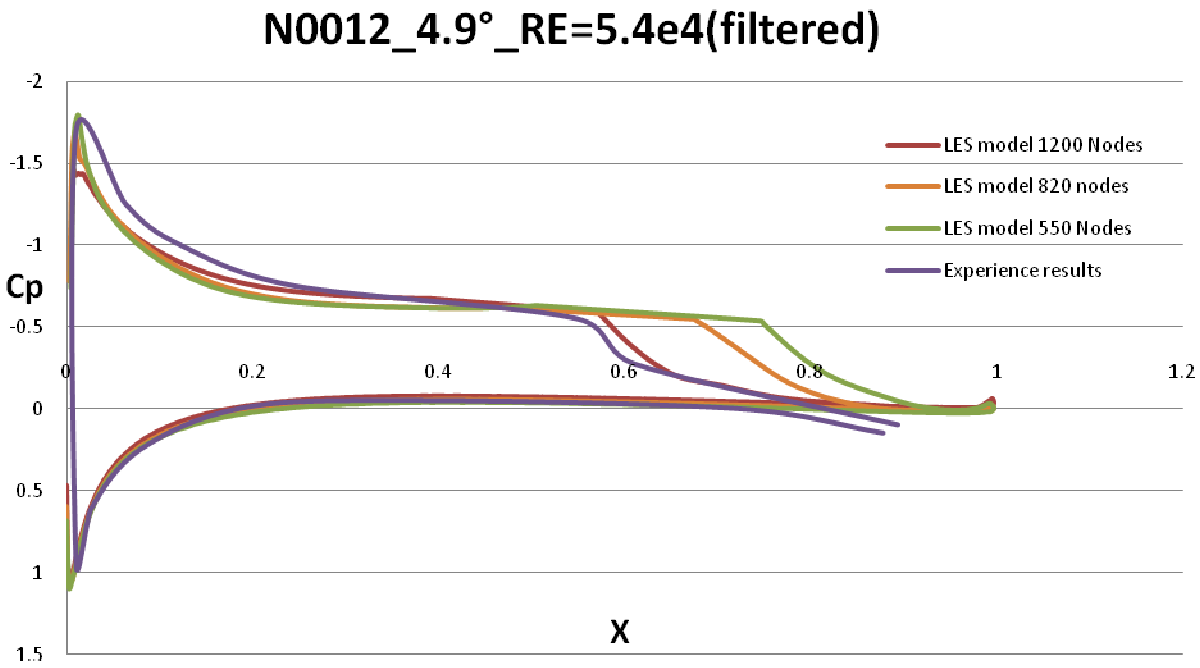

Figure 8 Behavior of the Cp for Various Mesh Sizes

The following table presents a summary of the different numerical results and errors obtained based on the laminar turbulent transition point for the same three different numbers of nodes:

Number of nodes on the airfoil fluid Structure Interface	**N_1=550**	**N_2=820**	**N_3=1200**
Refinement factor		N_2/N_1=1.49	N_3/N_2=1.46
Laminar-turbulent transition point position	0.753	0.679	0.574
Error when comparing with experiment	37.7%	25.2%	5.8%
Approximate relative error compared to the most refined mesh result	31.2%	18.3%	

Table 2 Comparison of the Results for Different Mesh Sizes

2D Wind Turbine

The next step of this study will be to explore the FSI features by studying the flow around a 2D wind turbine [5].

The first step to accomplishing this phase was to learn how the FSI features worked and to ensure that the meshing algorithm would correctly handle our rotating wind turbine problem.

The wind turbine structure will consist of three deformable NACA airfoils, regularly disposed at every 120° around a circle representing the diameter of the wind turbine (Figure 9). The junction between the airfoils and the inner tube of the wind turbine will be represented for simplification by rigid beams.

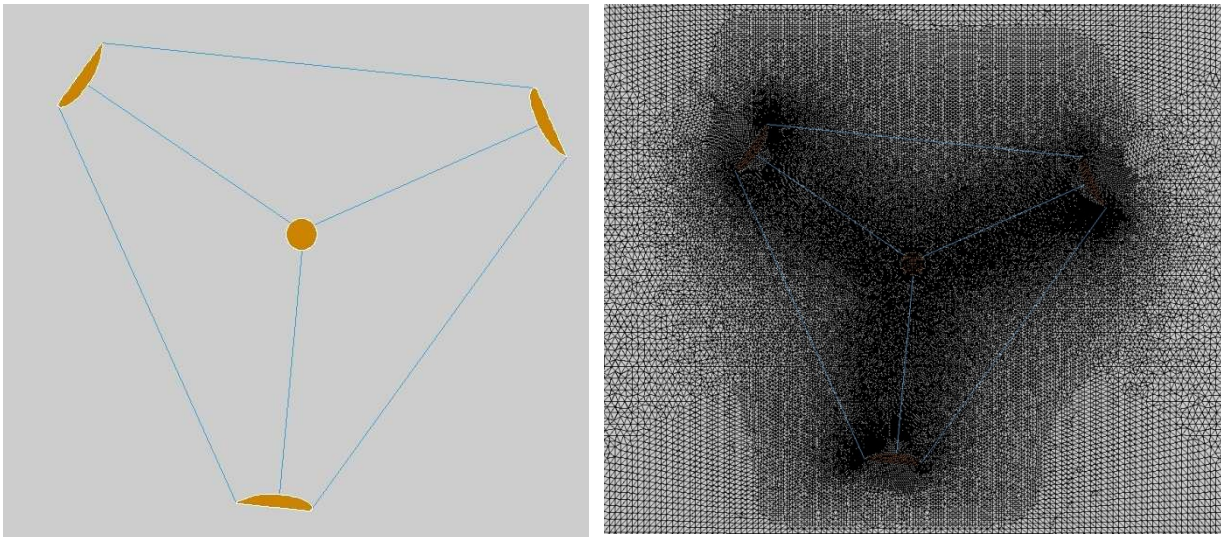

Figure 9 2D Geometry of the Wind Turbine and Corresponding Fluid Finite Element Mesh

Both the tube and the airfoils will have to interact with the incoming fluid. However, the beams are only there for convenience purposes and will therefore not be considered in the solving of the fluid-structure interactions problem. This can be done by only assigning the *ICFD_BOUNDARY_FSI keyword to the fluid parts that actually encircle the airfoils and the inner tube.

As we want to solve the complete fluid structure problem, we need both the fluid and the solid solver interacting with each other at each time step. Therefore, we will set the *ICFD_CONTROL_FSI keyword value to “0”.

The first preliminary tests have proven satisfactory with the structural and fluid solvers correctly interacting with one another.

An example of pressure and velocity fields obtained from LS-DYNA calculations is shown on Figure 10.

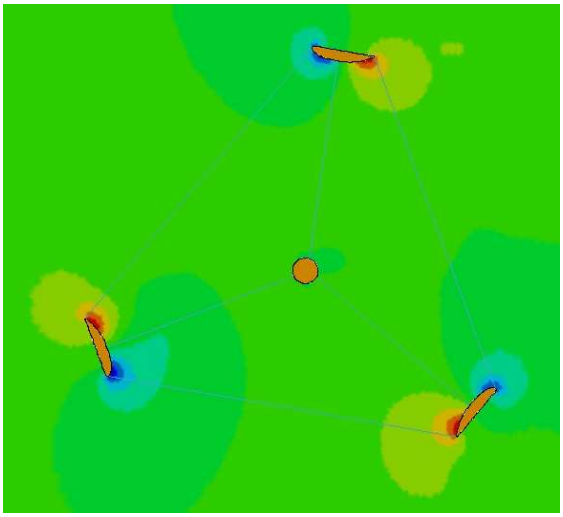

Figure 10.a Pressure Field

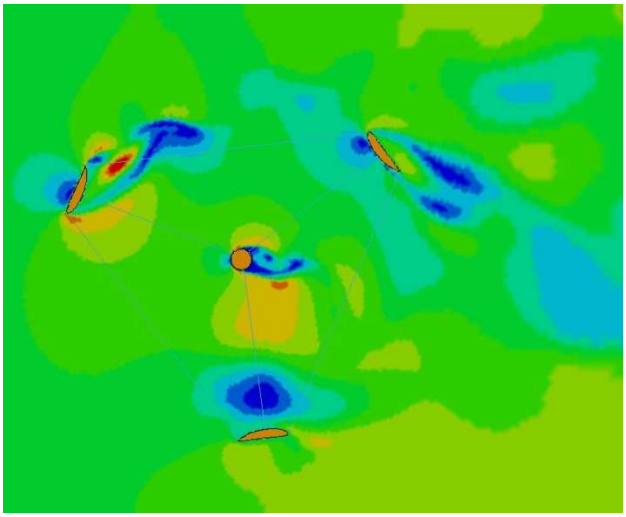

Figure 10.a Velocity Field

The next steps of this phase will be:

- To validate the 2D numerical results by comparing LS-DYNA results with results obtained using the CFD code STARCCM+.
- To run several 2D wind turbines models with various airfoil shapes in order to determine which ones offer the best aerodynamic behaviors.
- To simulate the complete 3D problem with the selected airfoils in order to assess the stress state in the different components of the wind turbine.

3D wind turbine

The last phase of this study will be to simulate the full 3D problem.

Some experimental tests were conducted in a wind tunnel with the current wind turbine in order to extract data about the rotating speed of the wind turbine as a function of the incoming wind speed. With the objective to validate the 3D model, we will try to obtain similar or approaching results. Then, the airfoils shapes that will have been selected by the 2D simulation will be tried in order to see if the results can be improved.

As for the 2D problem, preliminary simulations have been conducted in order to check if the solver was capable of handling such a complex geometry.

This way, we found out for instance that the initial meshing of the surfaces is essential for the automatic volume meshing algorithm to work correctly. Indeed, if the mesh is too coarse, it will have trouble recognizing boundaries with complex shapes such as the trailing edge of the airfoil (Figure 11). Fortunately, the solver allows the user to use the keywords *ICFD_CONTROL_SURFMESH enabling automatic surface re-meshing which aims at improving mesh quality on the boundaries. This code allows us to pursue the calculation of the 3D test case (Figure 12).

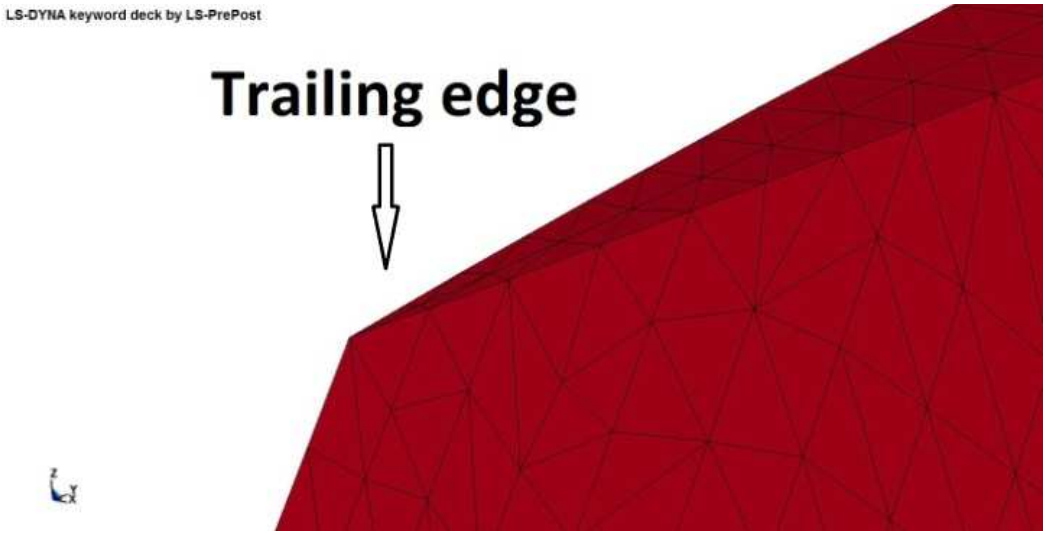

Figure 11 Zoom on a Trailing Edge of a 3D Wind Turbine Blade

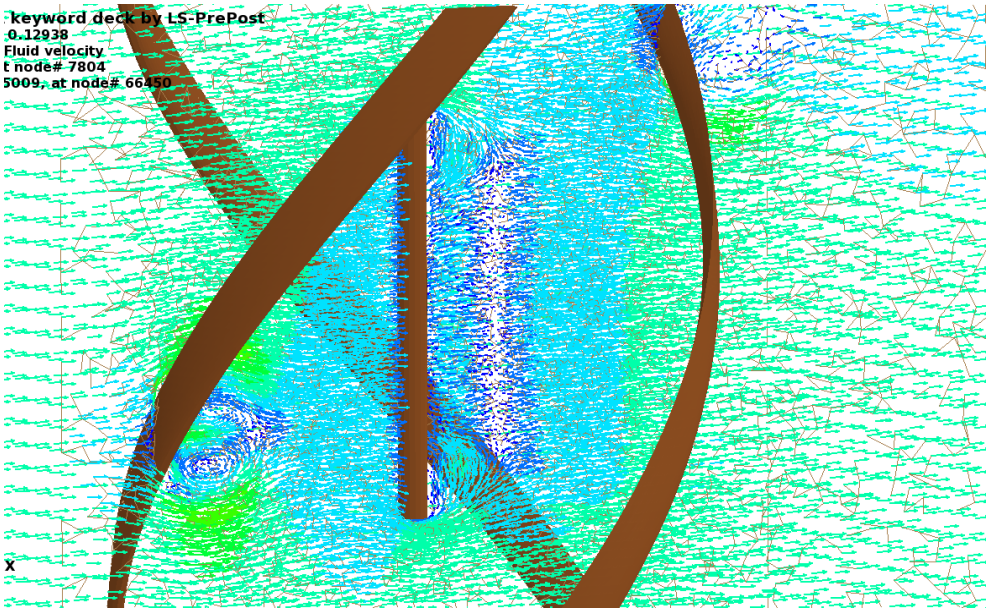

Figure 12 Velocity Vectors Visualization on a 3D Wind Turbine Case

Conclusion

The first results obtained during the validation process are encouraging and allow us to better understand the way the solver works. However, there are still a lot of investigations required such as trying to better understand the results concerning the Cd and Cl, or further studying the stalling. Furthermore, one must bear in mind that this solver is still a beta version and under development and that the results presented here may change along with future versions.

Concerning the 2D and 3D cases, the solver has proven to be capable of handling complex fluid-structure interactions such as the wind blowing on a wind turbine making the blades spin. After these first preliminary tests, we now feel confident enough to start with the next phase, i.e. running and comparing different 2D models before finally moving to the complete 3D model.

References

[1]Chassaing, P. (2000). *Mécanique des fluides.* Toulouse: CEPADUES EDITION.

[2] Oriol Guasch, R. C. (2007). *A heuristic argument for the sole use of numerical stabilization with no physical LES modeling in the simulatin of incompressible turbulent flows.* Barcelona: Universitat Politècnica de Catalunya.

[3]T.Lee, P. Gerontakos(2007). *Particle image velocimetry investigation of flow over unsteady airfoil with trailing edge strip.* Montreal: Mc Gill University.

[4] I. Celik *Procedure for Estimation and Reporting of Discretization Error in CFD Applications.* Morgantown: West Virginia university.

[5] S.R Idelsohn, F. Del Pin R. Rossi E.Oñate (2009). *Avoiding the instabilities caused by added mass effects in fluid structure interaction problems for pressure segregation and staggered approaches.* Barcelona: Universitat Politécnica de Catalunya.